Bioorganic & Medicinal Chemistry 17 (2009) 7615–7621

Contents lists available at ScienceDirect

Bioorganic & Medicinal Chemistry

journal homepage: www.elsevier.com/locate/bmc

Novel acenaphtho[1,2-*b*]pyrrole-carboxylic acid family: Synthesis, cytotoxicity, DNA-binding and cell cycle evaluation

Lijuan Xie [a], Yi Xiao [a], Fang Wang [b], Yufang Xu [b], Xuhong Qian [a,b,*], Rong Zhang [a], Jingnan Cui [a,*], Jianwen Liu [b,*]

[a] State Key Laboratory of Fine Chemicals, Dalian University of Technology, PO Box 89, 158 Zhongshan Road, Dalian 116012, China
[b] Shanghai Key Laboratory of Chemical Biology, School of Pharmacy, East China University of Science and Technology, PO Box 544, 130 Meilong Road, Shanghai 200237, China

ARTICLE INFO

Article history:
Received 8 December 2008
Revised 15 February 2009
Accepted 18 February 2009
Available online 23 February 2009

Keywords:
Acenaphtho[1,2-*b*]pyrrole
Cell cycle
Apoptosis
DNA

ABSTRACT

A family of 8-oxo-8*H*-acenaphtho[1,2-*b*]pyrrole-9-carboxylic acid derivatives were synthesized as a result of our efforts to modify a series of acenaphthopyrrole aromatic-heterocycle compounds that proved to be potent anticancer drugs. Among the derivatives, **3d** (3-(dimethylamino-propylamino)-8-oxo-8*H*-acenaphtho-[1,2-*b*]pyrrole-9-carboxylic acid) and **3g** (3-piperidine-8-oxo-8*H*-acenaphtho-[1,2-*b*]pyrrole-9-carboxylic acid) showed potential anticancer activity and different action mechanism from our previously reported compounds. UV–vis absorption, circular dichroism and viscosity measurement indicated that effect of both compounds on the advanced DNA conformation was different, although they could bind to DNA in the same way. Cell cycle analysis showed that **3d** could induce S-phase arrest followed by apoptosis, while **3g** induced apoptosis. The results seem to imply that different action mechanism could contribute to the dissimilitude of biological activities toward **3d** and **3g**.

1. Introduction

Uncontrolled cell proliferation and resistance to apoptosis are hallmarks of cancer.[1–4] Inhibit proliferation of cancer cell by blocking cell cycle progress or induction of apoptosis have emerged as an attractive approach for the treatment of cancer.[5–8] Anticancer drugs targeting DNA can inhibit cell cycle progression and/or induce apoptosis by activation of cell cycle checkpoint in response to DNA damage.[9–13] Thus, study of compounds that target DNA could not only develop new anticancer drugs, but also would provide a tool to understand regulatory network of cell proliferation and apoptosis.

In our previous work, the synthesis and biological evaluation for precursor **1**, **2** and **3a** (Fig. 1) have been reported, and the precursor exhibited strong anticancer activity in vitro and diversity of molecular target.[14–19] Based on the structure–activity relationship (SAR) study on the acenaphthopyrrole-heterocycle class, it seems that the electron-withdrawing group residing on chromophore are crucial to the anticancer activity and the slight structure modification of the chromophore or/and the substituted groups could change the mechanism of action and influence anticancer activity. The precursor **3a** is similar to **1a** and **2a** in structure, and the electron-withdrawing ability of carboxyl group is similar to that of carbonitrile and ester groups. It is well known that many drugs with nitrile or ester groups exert their effects through hydrolysis to the corresponding acid by enzymes.[20] Therefore, the better anticancer activities and new mechanism of action should be obtained by introduction of substituted groups into **3a**. In addition, the designed derivatives **3** should increase the solubility in water, which may be limit to exert the anticancer activity of **1** and **2**. We herein wish to report the design, synthesis, cytotoxic evaluation in vitro, DNA-binding study and analysis cell cycle of the new 8-oxo-8*H*-acenaphtho-[1,2-*b*]pyrrole-9-carboxylic acid derivatives with aliphatic amino substitution groups.

2. Results and discussion

2.1. Synthesis

The target compounds **3b–j** were obtained through the S_NAr^H reaction between precursor **3a**, which was prepared according to the report,[17] and nucleophilic reagents in DMF at room temperature, and the synthesis process and the yields were showed in Scheme 1 and Table 1, respectively. Although acetonitrile was chosen as the reaction solvent in previous synthesis of **1b–j** and **2b–j**, DMF was proved to be better than acetonitrile for synthesis of **3b–j**. It seems likely that the solubility of **3a** was improved and the S_NAr^H reaction could smoothly occur in DMF. The low yield of

* Corresponding authors. Tel.: +86 21 64253589; fax: +86 21 64252603 (X.Q.); tel.: +86 411 39893872; fax: +86 411 83673488 (J.C.); tel.: +86 21 64252044; fax: +86 21 64252044 (J.L.).
E-mail addresses: xhqian@ecust.edu.cn (X. Qian), jncui@dlut.edu.cn (J. Cui), liujian@ecust.edu.cn (J. Liu).

0968-0896/$ - see front matter © 2009 Elsevier Ltd. All rights reserved.
doi:10.1016/j.bmc.2009.02.031

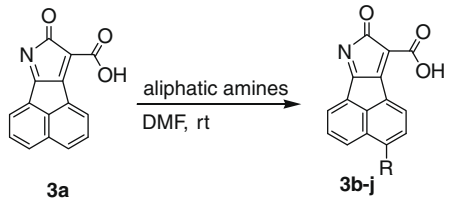

Scheme 1.

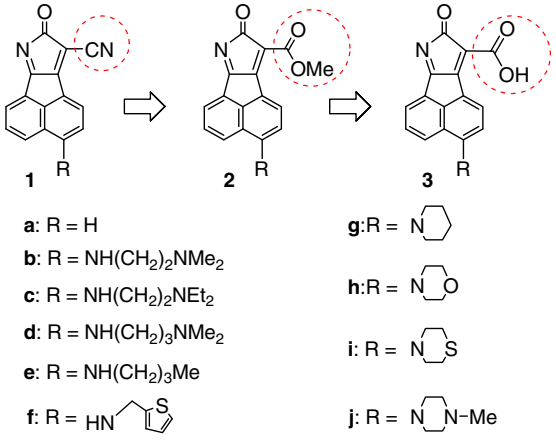

Figure 1.

the reaction is considered that the **3** is consumed as oxidizer similar to previous report.[15]

2.2. Cytotoxic evaluation in vitro

Cytotoxicity of the new derivatives against HeLa, HL-60, HCT-8, A375 and MCF-7 cell lines were evaluated by MTT[21] assay in vitro and were compared with the control compounds **1i** and **2i** as shown in Table 1. Among the compounds, **3g** is the most active, and **3f** and **3i** showed the weak active. Based on the previous reports, **1g** and **2g** present moderate anticancer activity, while **1f** and **1i** are the most active in the series of **1** and **2**.[15,17,19] The IC_{50} values of the most new derivatives against test cell lines are approximate or better to those of the control **1i** and stronger than that of the control **2i**. The results imply that electron-withdrawing groups residing on the chromophore are crucial to the anticancer activity and the new compounds could possess different action mechanism from series of **1** and **2.**

2.3. DNA-binding studies

To investigate the mechanism underlying the antiproliferative effect, the DNA-binding of **3d** and **3g** and their effect on cell cycle progression were studied, because the both compounds showed the different selective activity against tested cancer cell lines and kinds of substitution groups.

2.3.1. UV–vis absorption spectra studies

The UV–vis absorption spectra of **3d** with CT-DNA (calf thymus DNA) were firstly measured to examine the DNA-binding. As shown in Figure 2, the absorption titration spectra exhibited three changes suggesting cooperative effect between **3d** and DNA via intercalation and external contacts (surface binding). At $r < 0.5$ (r = [DNA]/[compound]), the obvious hypochromicity and slight red shift of short wavelength band were observed suggesting DNA-binding of **3d** by intercalation.[22] At $r = 0.5–1.0$, the almost unchanged absorbance could be associated with balance between intercalation and surface binding. The contrary absorbance change of the two wavelength band could support this conclusion, as shown in Figure 4 inset. At $r > 1$, hypochromicity of short wavelength band, the hyperchromicity of long wavelength band and obvious red shift were observed supporting the DNA-binding of **3d** through surface binding.[23,24] Absorption titration spectra between **3g** and CT-DNA is similar to that of **3d**.

Table 1
Cytotoxicity evaluation of the target compounds against HeLa, HL-60, HCT-8, A375 and MCF-7 cell clines in vitro

Compound	R	Yield[a] (%)	Cytotoxicity[b] (IC_{50}, μM)					K[c] (10^5 M^{-1})
			HeLa	HL-60	HCT-8	A375	MCF-7	
3b	$NH(CH_2)_2NMe_2$	20.2	89.72 ± 6.51	47.90 ± 3.43	>100	>100	97.02 ± 720	5.96 ± 0.09
3c	$NH(CH_2)_2NEt_2$	25.4	10.41 ± 1.06	19.83 ± 1.75	38.12 ± 2.53	71.81 ± 5.37	16.52 ± 1.54	5.48 ± 0.10
3d	$NH(CH_2)_3NMe_2$	27.3	29.32 ± 2.12	13.11 ± 1.41	>100	>100	70.52 ± 5.13	6.01 ± 0.12
3e	$NH(CH_2)_3Me$	26.4	30.33 ± 2.24	24.12 ± 2.06	48.12 ± 3.26	50.11 ± 3.45	>100	4.73 ± 0.07
3f	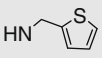	20.3	84.31 ± 5.98	90.02 ± 6.58	>100	>100	>100	6.75 ± 0.07
3g		40.2	20.61 ± 1.89	20.52 ± 1.78	24.42 ± 1.92	18.43 ± 1.61	14.51 ± 1.41	2.91 ± 0.06
3h		30.3	36.22 ± 2.35	42.21 ± 2.99	>100	79.41 ± 5.89	18.02 ± 1.67	2.34 ± 0.08
3i		26.7	48.91 ± 3.33	76.92 ± 5.87	>100	>100	>100	2.69 ± 0.56
3j		21.5	17.22 ± 1.57	51.03 ± 4.94	72.13 ± 5.24	28.51 ± 2.11	14.93 ± 1.56	6.13±0.14
1i			15.71 ± 1.41	28.62 ± 2.09	25.81 ± 2.04	48.71 ± 3.45	41.22 ± 3.21	
2i			26.92 ± 2.01	>100	>100	>100	68.03 ± 5.66	

[a] The yield was based on the consumed compound **3a**.
[b] Cytotoxicity (CTX) against HeLa (human cervical carcinoma), HL-60 (human promyelocytic leukemia cell), HCT-8 (human intestine ileocecal carcinoma cell), A375 (human melanoma cell) and MCF-7 (human breast tumor cell) were measured by MTT tetrazolium dye assay.[21]
[c] K: Intrinsic binding constant.

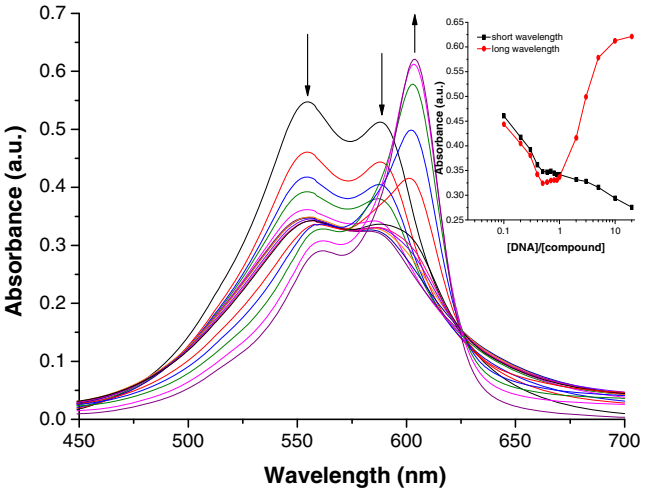

Figure 2. Titration absorption spectra of **3d** by CT-DNA in Tris–HCl buffer (pH 7.0), **3d** concentration is keeped in 30 μM and the DNA concentrations are varied from 3 μM to 30 μM in proportion, and then to 60, 90, 150, 300, and 600 μM. Inset: the absorbance in short wavelength band (555 nm) and long wavelength band (588 nm) of **3d** via the [CT-DNA]/[compound] ratio.

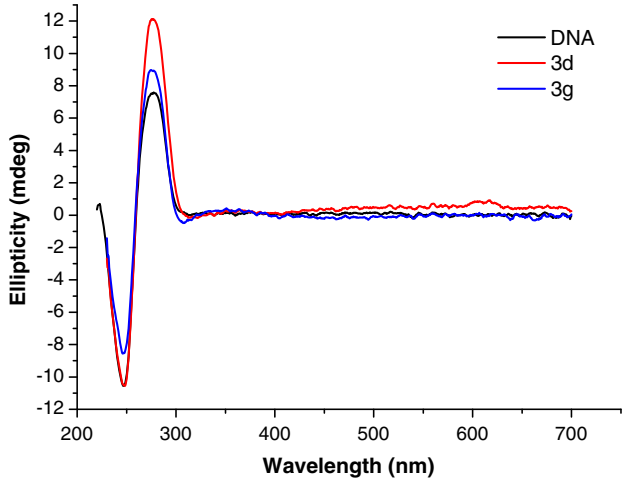

Figure 3. CD spectra of CT-DNA in the absence and presence of **3d** and **3g** at concentration of DNA 100 μM, and the concentration of **3d** and **3g** is 10 μM in Tris–HCl buffer (pH 7.0), respectively.

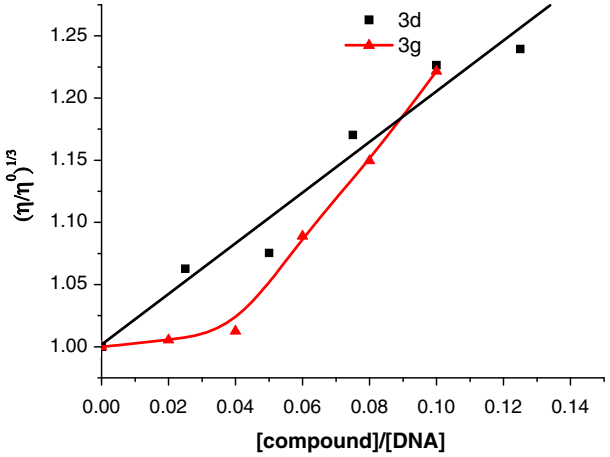

Figure 4. Effect of **3d** (■) and **3g** (▲) on the relative viscosities of CT-DNA at 25 (±0.1) °C. [DNA] = 100 μM. η is the viscosity of DNA in the presence of the compounds and η^o is the viscosity of DNA in the absence of the compounds.

The intrinsic binding constant, K, of a binding ligand to DNA can be determined from the ratio the of slop to intercept of a plot of $C_{DNA}/(\varepsilon_a - \varepsilon_f)$ against C_{DNA}.

$$C_{DNA}/(\epsilon_a - \epsilon_f) = C_{DNA}/(\epsilon_b - \epsilon_f) + 1/K(\epsilon_b - \epsilon_f)$$

where C_{DNA} is the concentration of DNA, ε_a = Aabs/[complex], ε_b and ε_f correspond to the extinction coefficients of DNA-bound complex and free complex, respectively. At r = 0.1–1.0 and 2–20, the K value is 6.01 × 105 and 0.90 × 105, respectively. The result supports the idea that 3d binds to DNA via intercalation and external contacts.

Comparing the IC_{50} and K data in Table 1, it was observed that there is no direct relationship between K and IC_{50} of the new derivatives. This means there is no direct relationship between DNA-binding and cytotoxicity. The results indicated that DNA is a potential, but not a unique, target for anticancer activity.

2.3.2. Circular dichroism spectra studies

CD (circular dichroism) is applied to understand the potential of **3d** and **3g** changing the DNA conformation as a very powerful technique to monitor the conformational state of the DNA double helix in solution.[25,26] As shown in Figure 3, the CD spectrum of free CT-DNA exhibited a negative band at 248 nm due to the helicity and a positive band at 278 nm due to the base stacking, which was the characteristic of DNA in the right-hand B form.[18] When the compounds were incubated with CT-DNA, the increases in the intensity of the positive band and the decrease in the intensity of the negative band with no distinct shift were observed, while the effect of **3d** on the base stacking was stronger and the effect of **3g** on the helicity was stronger. The influence of **3d** and **3g** on the advanced conformation of the DNA may be related to their substitution and lead to the different cytotoxicity.

A positive induced CD (ICD) signal of **3d** was observed, while induced CD signal was not detected in **3g**. Generally, a positive ICD indicates a perpendicular orientation of the transition dipole moment of the intercalated chromophore relative to the long axis of the intercalation pocket. ICD of the intercalated compound is dependent on the orientation of the transition moment inside the intercalation site, their lateral displacement relative to the helix axis and the type of base pairs forming the intercalation site.[27] The ICD difference between **3d** and **3g** could be attributed to the different steric demands and orientation relative to the binding pocket which results from the different substituted groups in **3g** and **3d**.

2.3.3. Viscosity measurement

Because viscosity measurement is regarded as a reliable tool to determine the binding model in solution in the absence of crystallographic structural data and NMR data,[22,25,26] the viscosity change of DNA after addition of **3d** or **3g** were also measured and showed in Figure 4. Intercalation of a molecule into DNA usually results in an increases in solution viscosity and the surface binding have a negligible effect on viscosity.[26] The increase in viscosity of DNA solution was observed versus the increase in concentration of **3d** and **3g** (Fig. 4), which could reflect a cooperative effect of the intercalation and surface binding. Based on the UV–vis absorption, circular dichroism and viscosity measurement, it can be concluded that effect of both compounds on the advanced DNA conformation was different, although they could bind to DNA in same way. Because many factors such as DNA itself, DNA-drug complex and environment could affect the UV-vis, CD spectra and viscosity when the compounds bind to CT-DNA, exact change of the conformation require further study.

2.4. Cell cycle evaluation

Previous studies have shown that compound **1i** and **1j** can induce apoptosis and **1d** neither arrest cell cycle nor induce apoptosis,[18] therefore the effect of compounds **3d** and **3g** on the cell cycle of HeLa cell lines was investigated by flow cytometry at various concentrations and showed in Figures 5 and 6. The cell cycle arrest or apoptosis was not observed after treatment with **3d** or **3g** at the 11.49 or 3.20 μM, for 24 and 36 h, respectively. Unexpectantly, the distinct S phase arrest (S 48.41% compared with control 28.20%) followed by apoptosis (apoptosis 13.89% compared with control 0) were observed after the incubation with **3d** in a concentration-dependent manner, while **3g** induced apoptosis (apoptosis 11.95% compared with control 0) for 48 h. The results could be attributed to the different influence of **3d** and **3g** on the advanced conformation of DNA.

3. Conclusion

The new acenaphthopyrrole carboxylic acid family is potential anticancer compounds and the study extends the SAR of the acenaphthopyrrole aromatic-heterocycle compounds. The DNA-binding studies indicated that compounds **3d** and **3g** could bind to DNA in the same way while their effect on the advanced DNA conformation was different. Cell cycle analysis showed that **3d** could induce S-phase arrest followed by apoptosis, while **3g** induced apoptosis. The precise mechanism of action is currently under way.

4. Experimental

All the solvents are of analytic grade. ^{1}H NMR and ^{13}C NMR spectra were measured on Bruker AV-500 and Bruker AV-400 spectrometer with chemical shifts reported in ppm (in DMSO-d_6, TMS as internal standard). Melting points were determined by using an X-6 micro-melting point apparatus and are uncorrected. Column chromatography was performed using silica gel 200–300 mesh. IR spectra were obtained using a Nicolet 470 FT-IR instrument. High-resolution mass spectra were obtained on a HPLC-Q-Tof Ms (Micro) instrument.

4.1. Synthesis

4.1.1. General procedure for the target compounds 3b–j

8-Oxo-8*H*-acenaphtho[1,2-*b*]pyrrol-9-carboxylic acid **3a** (0.5 mmol) which was prepared according to the report[17] and corresponding amines (2 mmol) in DMF (5 mL) were stirred at room temperature and detected by TLC. The solvent was removed under reduced pressure and the residue was subjected to column chromatography on silica gel. Products were separated with C_2H_5OH or CH_2Cl_2/MeOH (v/v) as a dark purple power.

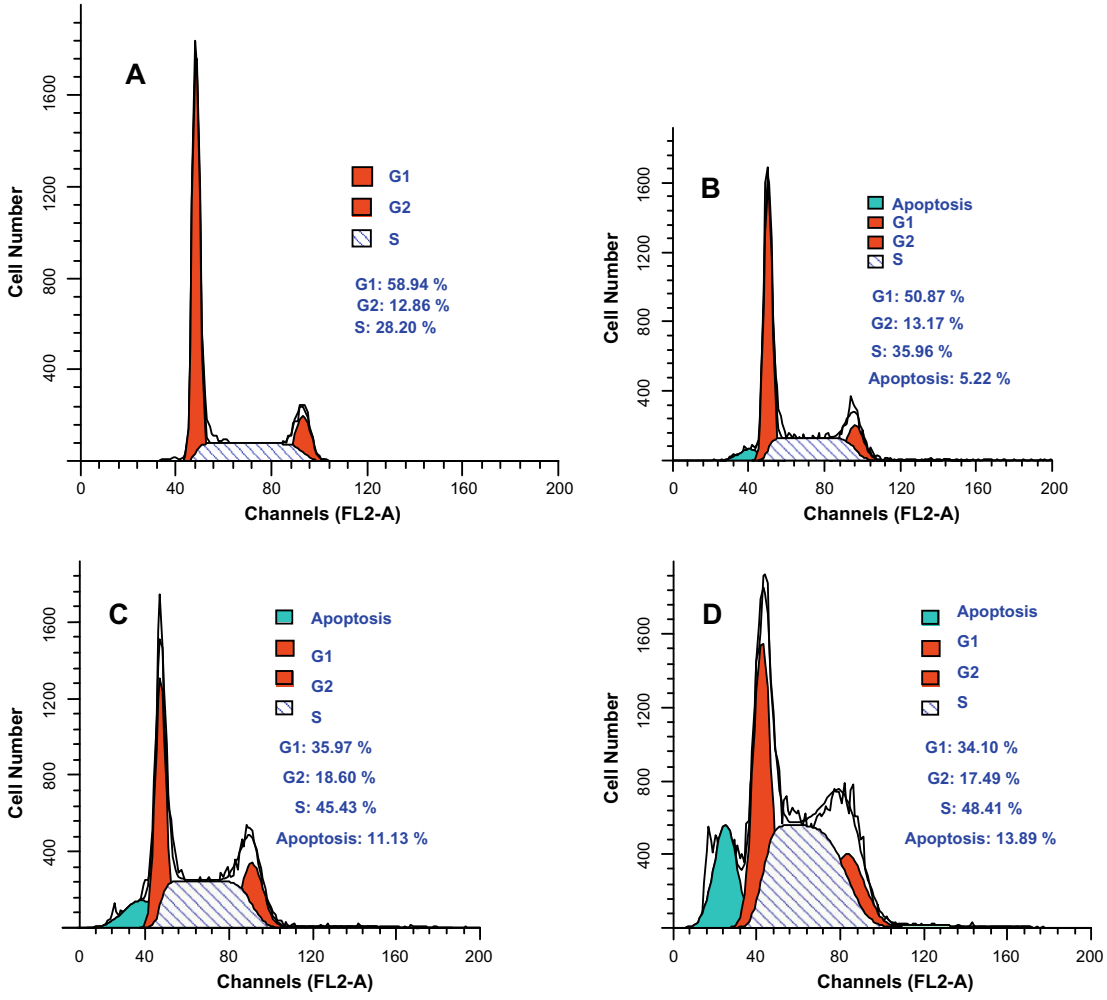

Figure 5. Cell cycle distribution determined by flowcytometry in HeLa cells treated with **3d** (A) 0 μM, (B) 11.46 μM, (C) 20.06 μM and (D) 28.65 μM.

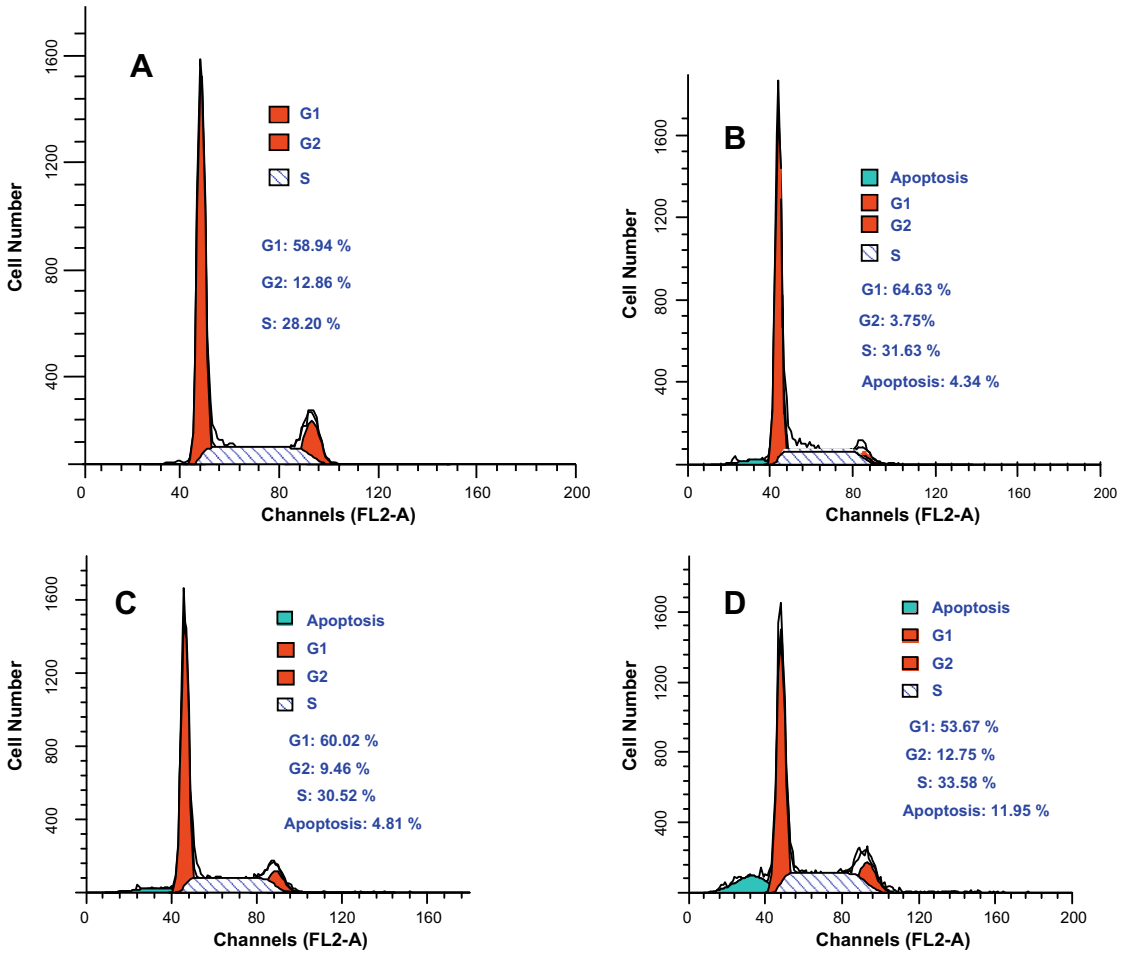

Figure 6. Cell cycle distribution determined by flowcytometry in HeLa cells treated with **3g** (A) 0 μM, (B) 3.01 μM, (C) 12.05 μM and (D) 21.08 μM.

4.1.2. 3-(2-Dimethylamino-ethylamino)-8-oxo-8*H*-acenaphtho[1,2-b]pyrrole-9-carboxylic acid (3b)

Yield 20.2%, mp > 300°C; ^{1}H NMR (400 MHz, DMSO-d_6) δ (ppm) 10.92 (s, 1H) 8.81 (t, 2H, J = 8.8 Hz) 8.59 (d, 1H, J = 8.0 Hz) 7.83 (t, 1H, J = 7.6 Hz) 6.98 (d, 1H, J = 8.0 Hz) 3.68 (t, 2H, J = 6.4 Hz) 2.78 (br, 2H) 2.36 (s, 6H); ^{13}C NMR (100 MHz, DMSO-d_6) δ (ppm) 175.9, 171.0, 169.1, 155.1, 141.7, 137.9, 133.7, 131.8, 130.8, 130.3, 126.2, 123.6, 115.8, 108.7, 107.8, 56.8, 45.4; IR (KBr cm^{-1}) 3237, 3081, 1710, 1614, 1573; HRMS (ESI) m/z (M-H)$^-$ calcd for $C_{19}H_{16}N_3O_3$ 334.1192, found: 334.1205.

4.1.3. 3-(2-Diehtylamino-ethylamino)-8-oxo-8*H*-acenaphtho[1,2-b]pyrrole-9-carboxylic acid (3c)

Yield 25.4%, mp 239–239.5°C; ^{1}H NMR (500 MHz, DMSO-d_6) δ (ppm) 8.79 (d, 2H, J = 8.4 Hz) 8.58 (d, 1H, J = 8.2 Hz) 7.83 (t, 1H, J = 8.0 Hz) 6.98 (d, 1H, J = 8.2 Hz) 3.63 (t, 2H, J = 6.0 Hz) 2.80 (br, 2H) 2.61 (br, 4H) 0.99 (t, 6H, J = 7.0 Hz); ^{13}C NMR (125MHz, DMSO-d_6) δ (ppm) 175.4, 170.6, 168.4, 154.8, 141.2, 137.5, 133.4, 131.4, 130.5, 129.6, 125.8, 123.2, 15.2, 108.1, 107.3, 50.6, 46.6, 11.6; IR (KBr cm^{-1}) 3251, 3049, 2977, 1740, 1703; HRMS (ESI) m/z (M−H)$^-$ calcd for $C_{21}H_{20}N_3O_3$ 362.1505, found: 362.1511.

4.1.4. 3-(3-Dimethylamino-propylamino)-8-oxo-8*H*-acenaphtho[1,2-b]pyrrole-9-carboxylic acid (3d)

Yield 27.3%, mp >300 °C; ^{1}H NMR (500 MHz, DMSO-d_6) δ (ppm) 8.78–8.76 (m, 2H) 8.57 (d, 1H, J = 8.0 Hz) 7.82 (t, 1H, J = 7.0 Hz) 6.94 (d, 1H, J = 8.0 Hz) 3.58 (t, 2H, J = 7.0 Hz) 2.57 (br, 2H) 2.33 (s, 6H) 1.94–1.91 (m, 2H); ^{13}C NMR (125 MHz, DMSO-d_6) δ (ppm) 175.5, 170.7, 168.6, 154.9, 141.3, 137.7, 133.5, 131.5, 130.5, 129.8, 126.0, 123.3, 115.2, 108.1, 107.2, 56.3, 44.6, 25.2; IR (KBr cm^{-1}) 3259, 3059, 1751, 1717, 1559; HRMS (ESI) m/z (M−H)$^-$ calcd for $C_{20}H_{18}N_3O_3$ 348.1348, found: 348.1337.

4.1.5. 3-Butylamino-8-oxo-8*H*-acenaphtho[1,2-*b*]pyrrole-9-carboxylic acid (3e)

Yield 26.4%, mp >300 °C; ^{1}H NMR (500 MHz, DMSO-d_6) δ (ppm) 10.91 (s, 1H) 8.87 (d, 1H, J = 7.9 Hz) 8.79 (d, 1H, J = 9.0 Hz) 8.59 (d, 1H, J = 7.9 Hz) 7.83 (t, 1H, J = 7.5 Hz) 6.96 (d, 1H, J = 9.0 Hz) 3.56–3.52 (m, 2H) 3.33 (br, 1H) 1.75–1.69 (m, 2H) 1.48–1.40 (m, 2H) 0.96 (t, 3H, J = 7.3 Hz); ^{13}C NMR (125 MHz, DMSO-d_6) δ (ppm) 175.3, 170.5, 168.4, 154.7, 141.2, 137.6, 133.4, 131.4, 130.4, 129.8, 125.7, 123.1, 115.0, 107.9, 107.1, 42.9, 32.1, 19.6, 13.6; IR (KBr cm^{-1}) 3259, 2955, 1751, 1717; HRMS (ESI) m/z (M−H)$^-$ calcd for $C_{19}H_{15}N_2O_3$ 319.1083, found: 319.1074.

4.1.6. 3-[(Thiophen-2-ylmethyl)-amino]-8-oxo-8*H*-acenaphtho[1,2-b]pyrrole-9-carboxylic acid (3f)

Yield 20.3%, mp >300°C; ^{1}H NMR (400 MHz, DMSO-d_6) δ (ppm) 10.15 (d, 1H, J = 6.0 Hz) 9.00 (d, 1H, J = 8.0 Hz) 8.64 (d, 1H, J = 7.2 Hz) 8.04 (d, 1H, J = 8.8 Hz) 7.95 (t, 1H, J = 8.0 Hz) 7.46 (d, 1H, J = 4.8 Hz) 7.22 (s, 1H) 7.15 (d, 1H, J = 9.2 Hz) 7.03–7.01 (m, 1H) 5.03 (d, 2H, J = 6.0 Hz); ^{13}C NMR (100 MHz, DMSO-d_6) δ (ppm) 177.4, 155.9, 140.1, 139.4, 133.3, 131.8, 130.2, 128.7, 127.9, 127.5, 127.2, 127.1, 126.4, 122.7, 116.4, 114.8, 112.4, 108.8, 106.0, 42.4; IR (KBr cm^{-1}) 3318, 1624, 1576, 1483; HRMS (ESI) m/z (M−H)$^-$ calcd for $C_{20}H_{11}N_2O_3S$ 359.0490, found: 359.0506.

4.1.7. 3-Piperidin-8-oxo-8*H*-acenaphtho[1,2-*b*]pyrrole-9-carboxylic acid (3g)

Yield 40.2% mp >300 °C; ^{1}H NMR (500MHz, DMSO-d_6) δ (ppm) 11.11 (s, 1H) 8.77 (d,1H, J = 8.5 Hz) 8.53 (dd, 1H, J = 1.0 and 7.5 Hz) 8.46 (dd, 1H, J = 1.0 and 7.5 Hz) 7.84 (t, 1H, J = 8.0 Hz) 7.27 (d, 1H, J = 8.5 Hz) 3.55 (t, 4H, J = 5.0 Hz) 1.83–1.81 (m, 4H) 1.73–1.72 (m, 2H); ^{13}C NMR (125 MHz, DMSO-d_6) δ (ppm) 176.7, 170.3, 168.1, 159.5, 141.9, 135.0, 133.2, 132.6, 131.1, 130.7, 126.0, 125.9, 119.2, 115.0, 112.2, 54.2, 25.6, 23.6; IR (KBr cm^{-1}) 3170, 3036, 1740, 1691; HRMS (ESI) m/z (M−H)$^-$ calcd for $C_{20}H_{15}N_2O_3$ 331.1083, found: 331.1089.

4.1.8. 3-Morpholin-8-oxo-8*H*-acenaphtho[1,2-*b*]pyrrole-9-carboxylic acid (3h)

Yield 30.3%, mp >300 °C; ^{1}H NMR (500 MHz, DMSO-d_6) δ (ppm) 11.19 (s, 1H) 8.86 (d, 1H, J = 8.5 Hz) 8.59 (d, 1H, J = 8.5 Hz) 8.56 (d, 1H, J = 8.0 Hz) 7.89 (t, 1H, J = 7.8 Hz) 7.36 (d, 1H, J = 8.0 Hz) 3.92 (t, 4H, J = 4.5 Hz) 3.50 (t, 4H, J = 4.5 Hz); ^{13}C NMR (125 MHz, DMSO-d_6) δ (ppm) 177.3 170.4 168.1 158.3 142.4 134.9 133.1 132.4 131.1 130.5 126.5 126.0 120.6 115.3 113.6 66.0 53.4; IR (KBr cm^{-1}) 3152, 3060, 1760, 1730, 1221; HRMS (ESI) m/z (M−H)$^-$ calcd for $C_{19}H_{13}N_2O_4$ 333.0875; found: 333.0861.

4.1.9. 3-Thiomorpholin-8-oxo-8*H*-acenaphtho[1,2-*b*]pyrrole-9-carboxylic acid (3i)

Yield 26.7%, mp >300 °C; ^{1}H NMR (500 MHz, DMSO-d_6) δ (ppm) 11.20 (s, 1H) 8.87 (d, 1H, J = 8.5 Hz) 8.58–8.55 (m, 2H) 7.91 (t, 1H, J = 8.5 Hz) 7.39 (d, 1H, J = 8.5 Hz) 3.72–3.70 (m, 4H) 2.98–2.96 (m, 4H); ^{13}C NMR (125 MHz, DMSO-d_6) δ (ppm) 206.3, 177.4, 170.4, 168.1, 159.1, 142.5, 134.8, 133.1, 132.3, 131.1, 130.4, 126.6, 120.9, 116.2, 113.9, 55.5, 30.6, 26.9; IR (KBr cm^{-1}) 3229, 3055, 1771, 1709; HRMS (ESI) m/z (M−H)$^-$ calcd for $C_{19}H_{13}N_2O_3S$ 349.0647; found: 349.0652.

4.1.10. 3-(4-Methyl-piperazin)-8-oxo-8*H*-acenaphtho[1,2-*b*]pyrrole-9-carboxylic acid (3j)

Yield 21.5%, mp >300 °C; ^{1}H NMR (500 MHz, DMSO-d_6) δ (ppm) 11.16 (s, 1H) 8.83 (d, 1H, J = 8.5 Hz) 8.56 (dd, 1H, J = 1.0 and 8.5 Hz) 8.53 (dd, 1H, J = 1.0 and 8.5 Hz) 7.88 (t, 1H, J = 8.0 Hz) 7.34 (d, 1H, J = 8.5 Hz) 3.55 (t, 4H, J = 4.7 Hz) 2.66 (br, 4H) 2.32 (s, 3H); ^{13}C NMR (125 MHz, DMSO-d_6) δ (ppm) 177.1, 170.4, 168.1, 158.5, 142.3, 134.9, 133.1, 132.5, 131.1, 130.6, 126.3, 125.9, 120.1, 115.3, 113.1, 54.4, 52.9, 45.4, 30.6; IR (KBr cm^{-1}) 3537, 1745, 1704; HRMS (ESI) m/z (M−H)$^-$ calcd for $C_{20}H_{16}N_3O_3$ 346.1192; found: 346.1203.

4.2. Cytotoxic evaluation in vitro

HeLa, HL-60, HCT-8, A375 and MCF-7 cells were seeded into 96-well microculture plates and allowed to adhere for 24 h (8 h for HeLa). After cells were exposed to compounds at concentrations from 100 to 0.01 μM for 48 h, medium was aspirated and replenished with complete medium. IC_{50} was evaluated by MTT tetrazolium dye assay.[21] Each experiment was performed three times.

4.3. DNA-binding studies

UV–vis absorption spectra were recorded on a PGENERAL TU-1901 UV–vis spectrophotometer and fluorescent spectra were measured on a Hitachi F-4500 luminescence spectrophotometer. Calf-thymus (CT) DNA was purchased from the Sino–American Biotechnology Company. Solution of CT-DNA in Tris–HCl buffer (30 mM, pH 7.5) gave a ratio of UV absorbance at 260 and 280 nm of 1.8–1.9:1, indicating that the DNA was sufficiently free from protein. The concentration of CT-DNA was determined by its absorption intensity at 260 nm with a known molar absorption coefficient value of 6600 M^{-1} cm^{-1}.

4.3.1. UV–vis absorption spectra studies

The titration absorption spectra studies were performed by keeping constant the concentration of compound while varying the DNA concentration at room temperature. Initially, solutions of the blank buffer were placed in the reference and sample cuvettes (1 cm path length), respectively, and then the first spectrum was recorded in the range 200–650 nm. During the titration, aliquots of buffered DNA solution were added and the solutions were mixed by repeated inversion. After mixing for 10 min, the absorption spectra were recorded. The titration processes were repeated until there was no change in the spectra for at least four titrations indicating binding saturation had been achieved.

4.3.2. Circular dichroism spectra studies

The CD (circular dichroism) spectra were scanned with a J-810 spectrophotometer (Jasco, Japan) using a 1-cm path quartz cell and subtracted from the spectrum of Tris–HCl buffer alone. The CD spectra were recorded at the compound concentration of 10 μM and DNA concentration of 100 μM, in the region 200–700 nm.

4.3.3. Viscosity experiments

Calf-thymus DNA was dissolved in Tris–HCl buffer (30 mM, pH 7.5) and left at 4 °C overnight. It was treated in an ultrasonic bath for 10 min, and the solution was filtered through a PVDF membrane filter (pore size of 0.45 μm) to remove insoluble material, the concentration of CT-DNA was 100 μM. Viscometric titrations were performed with an Ubbelodhe viscometer immersed in a thermostated bath maintained 25 (±0.1) °C. The flow times were measured with a digital stopwatch, each sample was measured three times, and an average flow time was calculated. Data are presented as $(\eta/\eta^0)^{1/3}$ versus [complex]/[DNA], where η is the viscosity of DNA in the presence of complex and η^0 is the viscosity of DNA alone. Viscosity values were calculated from the observed flowing time of DNA-containing solutions (t) corrected for that of the buffer alone (t_0), $\eta = (t - t_0)$.

4.4. Flow cytometric analysis of cellular DNA content

Flow cytometric analysis of cellular DNA content was performed as described follow. Cells (1×10^5/mL) were seeded in a 6-well culture plate, after 24 h incubation, cells were treated with 0, 1, 4, 7 and 10 μg/mL of **3d** and **3g** for 0, 12, 24, 36, and 48 h, respectively. Both floating and attached cells were collected and poured together in the centrifuge tubes. Cells were washed three times with phosphate-buffered saline (PBS), re-suspended and fixed in 70% ice-cold ethanol for 2 h at 4 °C. Subsequently they were re-washed two times with phosphate-buffered saline (PBS) and treated with RNase A (100 μg/mL) and propidium iodide (PI) (20 μg/mL) for 30 min in the dark. Finally, cells were analyzed in a FACScan flow cytometer (Becton Dickinson, USA). The percentage of cells in G_0/G_1 phase, S phase, G_2/M and sub-G_1 phase was analyzed using standard MODIFIT and CELLQUEST software programs.

Acknowledgments

We are grateful to the National Key Project for Basic Research (2003CB114400) and the National Natural Science Foundation of China (20536010).

References and notes

1. Okada, H.; Mak, T. W. *Nat. Rev. Cancer* **2004**, *4*, 592.
2. Besson, A.; Assoian, R. K.; Roberts, J. M. *Nat. Rev. Cancer* **2004**, *4*, 948.

3. Fesik, S. W. *Nat. Rev. Cancer* **2005**, *5*, 876.
4. Nakayama, K. I.; Nakayama, K. *Nat. Rev. Cancer* **2006**, *6*, 369.
5. Evan, G. I.; Vousden, K. H. *Nature* **2001**, *41117*, 342.
6. Malumbres, M.; Barbacid, M. *Nat. Rev. Cancer* **2001**, *1*, 222.
7. Senderowicz, A. M. *Curr. Opin. Cell. Biol.* **2004**, *16*, 670.
8. Rodriguez-Nieto, S.; Zhivotovsky, B. *Curr. Pharm. Des.* **2006**, *12*, 4411.
9. Hartwell, L. H.; Weinert, T. A. *Science* **1989**, *246*, 629.
10. Prudhomme, M. *Curr. Med. Chem. Anti-Cancer Agents* **2004**, *4*, 435.
11. Zhou, B.-B. S.; Bartek, J. *Nat. Rev. Cancer* **2004**, *4*, 1.
12. Kastan, M. B.; Bartek, J. *Nature* **2004**, *432*, 316.
13. Tao, Z.; Lin, N. *Anti-Cancer Agents. Med. Chem.* **2006**, *6*, 377.
14. Xiao, Y.; Liu, F.; Qian, X.; Cui, J. *Chem. Commun.* **2005**, 239.
15. Liu, F.; Xiao, Y.; Qian, X.; Zhang, Z.; Cui, J.; Cui, D.; Zhang, R. *Tetrahedron* **2005**, *61*, 1126.
16. Zhang, Z.; Yang, Y.; Liu, F.; Qian, X.; Xu, Q. *Int. J. Biol. Macromol.* **2006**, *38*, 59.
17. Liu, F.; Qian, X.; Cui, J.; Xiao, Y.; Zhang, R.; Li, G. *Bioorg. Med. Chem.* **2006**, *14*, 4639.
18. Zhang, Z.; Yang, Y.; Zhang, D.; Wang, Y.; Qian, X.; Liu, F. *Bioorg. Med. Chem.* **2006**, *14*, 6962.
19. Zhang, Z.; Jin, L.; Qian, X.; Wei, M.; Wang, Y.; Wang, J.; Yang, Y.; Xu, Q.; Xu, Y.; Liu, F. *Chem. Bio. Chem.* **2007**, *8*, 113.
20. Hyatt, J. L.; Wadkins, R. M.; Tsurkan, L.; Hicks, L. D.; Jason Hatfield, M.; Edwards, C. C.; Ross, C. R., II; Cantalupo, S. A.; Crundwell, G.; Danks, M. K.; Kip Guy, R.; Potter, P. M. *J. Med. Chem.* **2007**, *50*, 5727.
21. Kuroda, M.; Mimaki, Y.; Sashida, Y.; Hirano, T.; Oka, K.; Dobashi, A.; Li, H.; Harada, N. *Tetrahedron* **1997**, *53*, 11549.
22. Ihmels, H.; Otto, D. *Top. Curr. Chem.* **2005**, *258*, 161.
23. Wu, L.; Teng, H.; Ke, X.; Xu, W.; Su, J.; Liang, S.; Hu, X. *Chem. Biodivers.* **2007**, *4*, 2198.
24. Taima, H.; Okubo, A.; Yoshioka, N.; Inoue, H. *Chem. Eur. J.* **2006**, *12*, 6331.
25. Palchaudhuri, R.; Hergenrother, P. J. *Curr. Opin. Biotechnol.* **2007**, *18*, 497.
26. Wheate, N. J.; Brodie, C. R.; Collins, J. G.; Kemp, S.; Aldrich-Wright, J. R. *Mini-Rev. Med. Chem.* **2007**, *7*, 627.
27. Eriksson, M.; Norden, B. *Drug–Nucleic Acid Interact.* **2001**, *340*, 68.